Magnetic and Optical Properties of Poly(vinylidene difluoride)/Fe_3O_4 Nanocomposite Prepared by Coprecipitation Approach

Chunhua Xu, Chunfa Ouyang, Runping Jia, Yongsheng Li, Xia Wang

Department of Materials Science and Engineering, Shanghai Institute of Technology, Shanghai 200235, People's Republic of China

Received 6 March 2008; accepted 25 August 2008
DOI 10.1002/app.29194
Published online 30 October 2008 in Wiley InterScience (www.interscience.wiley.com).

ABSTRACT: Poly(vinylidene difluoride) (PVDF)/Fe_3O_4 magnetic nanocomposite was prepared by a simple coprecipitation method, and was characterized by scanning electron microscope (SEM), X-ray diffraction (XRD), vibrating sample magnetometer (VSM), and ultraviolet visible spectroscopy (UV-Vis). The SEM images showed that Fe_3O_4 nanoparticles were dispersed in the PVDF matrix as some aggregates with the sizes of 50 nm–2 μm, and the XRD curves showed the incorporation of the Fe_3O_4 nanoparticles in PVDF matrices and the decrease of the crystallinity of the PVDF. VSM results showed that the saturation magnetization (M_s) and remnant magnetization (M_r) of the PVDF/Fe_3O_4 nanocomposite increased with the increase of the Fe_3O_4 content, and that M_s and M_r along the parallel direction were higher than those along the perpendicular direction at the same Fe_3O_4 content. The coercive force (H_c) of the nanocomposite was independent of the Fe_3O_4 content and approximately equal along the parallel and perpendicular direction at the same Fe_3O_4 content. The optical band gap (E_g) of the PVDF/Fe_3O_4 nanocomposite was influenced by the Fe_3O_4 content, and decreased by 0.75 eV compared with that of pure PVDF when the Fe_3O_4 content was 3 wt %. © 2008 Wiley Periodicals, Inc. J Appl Polym Sci 111: 1763–1768, 2009

Key words: poly(vinylidene difluoride) (PVDF); Fe_3O_4; nanocomposite; magnetization property; optical property

INTRODUCTION

Magnetic polymer materials represent a class of functional materials, which may have some potential applications in batteries, electrochemical display devices, electromagnetic interference shielding, electromagneto-rheological fluids, microwave-absorbing materials, magnetic separations, enzyme immunoassay, drug targeting, and so on.[1–9] In recent years, studies on the preparation and properties of various magnetic polymer composite have attracted more and more attention. For example, Chen et al.[10,11] studied the electrical and magnetic properties of polypyrrole-Fe_3O_4 nanocomposite by modifying the surfaces of the Fe_3O_4 nanoparticles with ethanol and Fe^{3+} before emulsion polymerization in the presence of surfactant sodium dodecyl sulfate. Qiu et al.[12] prepared polystyrene (PS)/Fe_3O_4 magnetic emulsion and nanocomposite by ultrasonically initiated miniemulsion polymerization and studied their structure, morphology, and magnetic properties. Kaise et al.[13] studied electronic transport properties of conducting polyaniline and polymer blends. Lee et al.[14] prepared nanocomposite Langmuir-Blodgett films of poly(maleic monoester) (PMA)/Fe_3O_4 nanoparticles and studied the dispersion of Fe_3O_4 nanoparticles between poly(maleic monoester) layers, surface morphology of the nanocomposite film, and magnetic properties. These magnetic polymer composites were prepared by methods such as polymerization,[2,10,12] blending,[13,15] and sol-gel.[14,16]

In this work, poly(vinylidene difluoride) (PVDF)/Fe_3O_4 magnetic nanocomposite was prepared by a simple coprecipitation method with the aid of ultrasonic technique. PVDF is a multipurpose polymer used in piezoelectric and pyroelectric materials, nonlinear optics, microwave transducers, ultrafiltration membrane, biomedical fields, dyesensitized solar cells as a solid polymer electrolyte, and so on;[17–21] therefore, it can be very interesting to combine the unique properties of PVDF and magnetic Fe_3O_4 nanoparticles to prepare the nanocomposite. So far as we know, no detailed investigation on the preparation of such a magnetic nanocomposite by coprecipitation has been reported in the literature.

Correspondence to: C. Xu (chhxu@sit.edu.cn).
Contract grant sponsor: Key Subject Construction Project in Shanghai; contract grant number: p1502.
Contract grant sponsor: Foundation of the Shanghai Institute of Technology; contract grant number: YJ2007-37.

PVDF/Fe_3O_4 nanocomposite with unique magnetic properties would find their potential applications in electromagnetic shielding, microwave-absorbing materials, and so on.

EXPERIMENTAL

Material

Fe_3O_4 nanoparticles were purchased from Ma-An-Shan Jinke powder engineer company, Anhui, P. R. China. PVDF (M = 400,000–600,000) was purchased from Shanghai 3F new materials company, Shanghai, P. R. China. Other reagents used in the experiments were all analytical grade such as N,*N*-dimethylacetamide (DMAc) and anhydrous ethanol.

Preparation of PVDF/Fe_3O_4 nanocomposite

Firstly, appropriate amounts of PVDF and Fe_3O_4 nanoparticles were measured out for the desired weight fractions, and then separately, the PVDF particles was dissolved and Fe_3O_4 nanoparticles were dispersed in DMAc by magnetic stirrer and sonication for about 60 min. Next, the PVDF-DMAc solution and Fe_3O_4-DMAc disperse liquid were mixed together and sonicated for about 30 min. Then, the mixtures were poured slowly into the deioned water as nonsolvent to coprecipitate PVDF/Fe_3O_4 nanocomposite. After filtration, the recovered nanocomposite was washed using water and anhydrous ethanol in sequence to remove the residual DMAc and water in the nanocomposite. Finally, the flocculent nanocomposite was vacuum-desiccated for about 5 h at 70°C, afterward, the floc was hot-pressed for 10 min at 180°C under 10 MPa pressure to get 65–85 μm thin slices.

Characterization

The sizes and structure of Fe_3O_4 were characterized by transmission electron microscope (TEM) using JEOL-200CX operated at 200 kV. The fracture sections and dispersion state of the Fe_3O_4 nanoparticles in PVDF matrices were observed by scanning electron microscope (SEM) using Hitachi *S*-4500. The fracture samples were gained by cooling and breaking the slices in liquid nitrogen, and were coated with carbon for SEM analysis. X-ray diffraction (XRD) of the samples was performed with a Bruker D8-Advance diffractometer using Cu K_α radiation, to assess the structural changes of the nanocomposite in the presence of the Fe_3O_4 nanoparticles. The magnetization curves were recorded by vibrating sample magnetometer (VSM) using a Riken-Denshi BHV-50HTI in magnetic fields up to 15 kOe at room temperature, to analyze the saturation magnetization (M_s) and remnant magnetization (M_r). In this work, the parallel and perpendicular magnetic properties were comparatively studied; the "parallel and perpendicular" meant that the direction of magnetic field was separately parallel and perpendicular to the surfaces of the thin slices. Because of the partially inhomogeneous dispersion of the Fe_3O_4 nanoparticles in PVDF matrices, the accurate mass of Fe_3O_4 nanoparticles in each sample was measured by inductively coupled plasma-atomic emission spectrometer (ICP-AES) using a Perkin–Elmer Optima 3300RL. The ultraviolet visible spectra (UV-Vis) were recorded with a Shimadzu UV-2100 instrument, and the data were analyzed to determine the changes of the absorption coefficients and optical band gap (E_g) with the content of the Fe_3O_4 nanoparticles in PVDF matrix.

RESULTS AND DISCUSSION

Morphology analysis

Figure 1(a) shows the TEM image and electrical diffraction pattern of the Fe_3O_4 nanoparticles. It can be seen that the sizes of the Fe_3O_4 nanoparticles concentrate on about 10–20 nm, and that the nanoparticles have a polycrystalline structure indicated by the inserted electrical diffraction. Figure 1(b–d) shows the SEM images of the fracture surfaces of the pure PVDF and nanocomposite slices with 5 and 30 wt % Fe_3O_4. A contrast analysis of the SEM images of the pure PVDF [Fig. 1(b)] and the nanocomposite [Fig. 1(c,d)] indicates that Fe_3O_4 particles are dispersed into the PVDF matrices shown as white parts in gray PVDF matrices. From the scale bars, it can be seen that the sizes of the Fe_3O_4 particles in the PVDF matrices are 50–500 nm in Figure 1(c) and 200 nm–2 μm in Figure 1(d), respectively. These Fe_3O_4 particles in PVDF matrices are much bigger than the pristine Fe_3O_4 nanoparticles; moreover, the Fe_3O_4 particles in the PVDF matrices turn big with the increase of the Fe_3O_4 content [Fig. 1(c,d)]. These show that most of the Fe_3O_4 nanoparticles form some aggregates in the PVDF matrices. When the Fe_3O_4 content is lower than 1 wt %, the Fe_3O_4 aggregates can not be observed under the SEM, which indicates a better dispersion of the Fe_3O_4 nanoparticles in PVDF matrix. Altogether, the dispersion state of the Fe_3O_4 nanoparticles in PVDF matrix is related to their content. The higher the Fe_3O_4 content, the more aggregated are the Fe_3O_4 nanoparticles.

X-ray diffraction analysis

Figure 2 shows XRD patterns of the Fe_3O_4 nanoparticles, pure PVDF, and nanocomposite slices with different Fe_3O_4 content. The diffraction peaks of

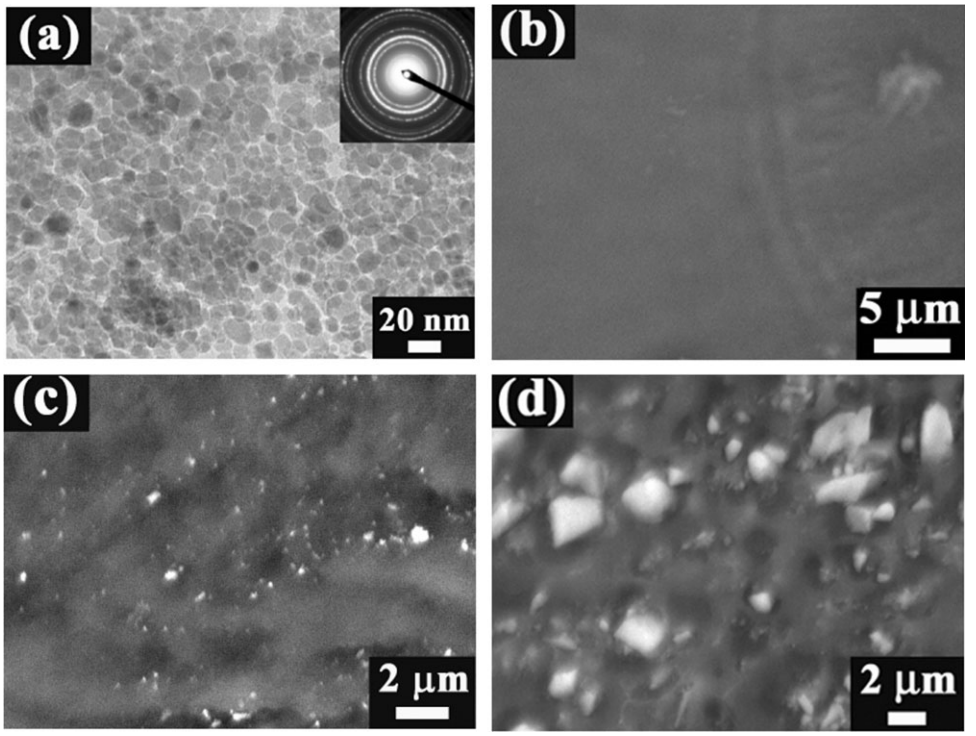

Figure 1 (a) TEM image of Fe_3O_4 nanoparticles and the inserted electric diffraction pattern; fracture SEM image of (b) pure PVDF, (c) PVDF/Fe_3O_4 nanocomposite with 5 wt % Fe_3O_4, and (d) PVDF/Fe_3O_4 nanocomposite with 30 wt % Fe_3O_4.

Fe_3O_4 nanoparticles at 30.1°, 35.5°, 43.1°, 53.5°, 57.0°, and 62.6° corresponding to (220), (311), (400), (422), (511), and (440) planes indicate that the Fe_3O_4 nanoparticles have a cubic spinel structure.[22,23] The diffraction peaks of the nanocomposite at 30.0° and 62.2° become more and more prominent with the increase of the Fe_3O_4 content, and the diffraction peaks at 35.0° and 42.6° turn more intense and broader. These results are attributed to the characteristic diffraction of the Fe_3O_4 nanoparticles and prove the incorporation of the Fe_3O_4 nanoparticles in PVDF matrices. The diffraction curve of pure PVDF shows that it is partially crystalline with its characteristic diffraction peaks at 32.6°, 38.9°, 47.1°, and 48.1°. However, these characteristic peaks turn weak with the increase of the Fe_3O_4 content, which indicates that the addition of Fe_3O_4 nanoparticles decreases the crystallinity of PVDF in the nanocomposite.[2] On the other hand, there is no new peak found in diffractive curves except for those of the PVDF and the Fe_3O_4 particles, which shows that there is no new phase produced.

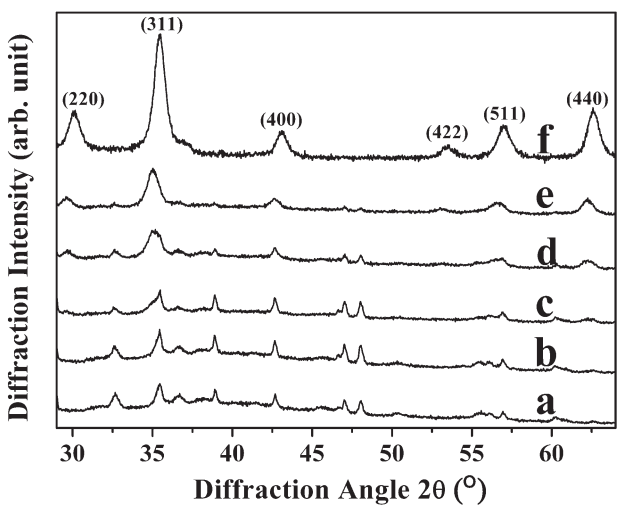

Figure 2 XRD patterns of (a) pure PVDF, PVDF/Fe_3O_4 nanocomposite with (b) 1 wt % Fe_3O_4, (c) 5 wt % Fe_3O_4, (d) 10 wt % Fe_3O_4 and (e) 30 wt % Fe_3O_4, and (f) XRD patterns of the Fe_3O_4 nanoparticles.

Magnetic properties analysis

The magnetic properties of the nanocomposite were measured by VSM. Figure 3 shows the variation of the parallel and perpendicular M_s and M_r of the PVDF/Fe_3O_4 nanocomposite with the Fe_3O_4 content. From the curves, it can be seen that M_s and M_r of the nanocomposite increase with the increase of Fe_3O_4 content, and M_s and M_r along the parallel are higher than those along the perpendicular at the same Fe_3O_4 content. When the Fe_3O_4 content increases from 0.1 to 30 wt %, the M_s increases from about 4.1 to 48.2 emu/g along the parallel and about 5.1 to 37.8 emu/g along the perpendicular, and the corresponding M_r increases from about 0.4 to 6.1 emu/g and about 0.3 to 2.8 emu/g, respectively.

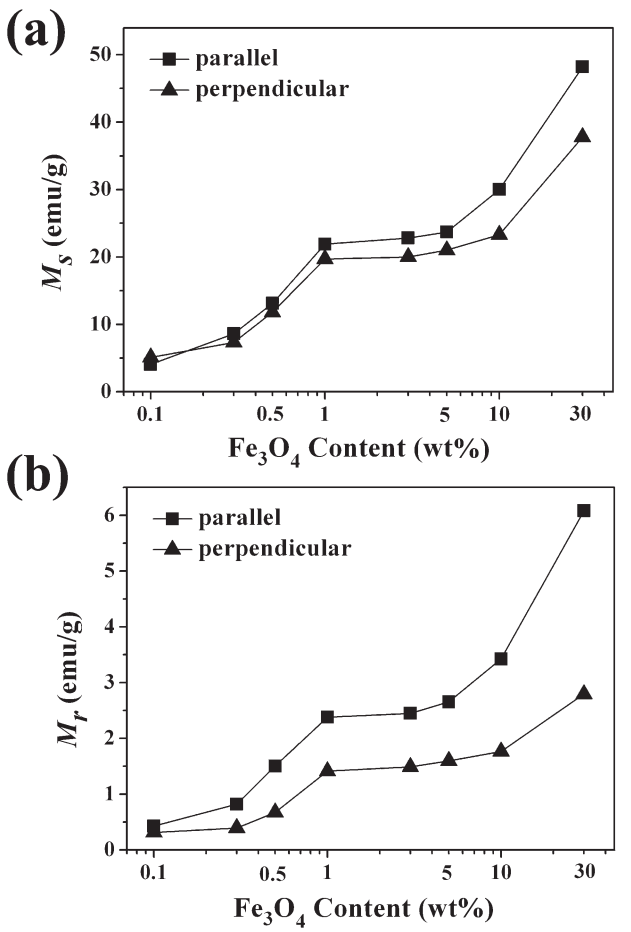

Figure 3 Variation of (a) the parallel and perpendicular saturation magnetization (M_s) and (b) parallel and perpendicular remnant magnetization (M_r) of the PVDF/Fe_3O_4 nanocomposite slices with the Fe_3O_4 content.

These results probably are related to the state of dispersion and aggregation of the Fe_3O_4 nanoparticles in PVDF matrices.[24] When the Fe_3O_4 content is low, the nanoparticles are dispersed well in PVDF matrix and the magnetic domain is probably not easy to form, which causes a low saturation magnetization. With the increase of the Fe_3O_4 content, the Fe_3O_4 nanoparticles tend to aggregate [Fig. 1(b,c)] and thus, more magnetic domains form, so the M_s increases.[11] Although more magnetic domains are formed at the higher Fe_3O_4 content, more magnetic domains are probably remained when the magnetic field intensity is zero, which may lead to the higher M_r, so the M_r shows a similar variation law with M_s. On the other hand, the difference of M_s and M_r along the parallel and perpendicular direction may be related to the anisotropy of the slices resulted from the hot-pressed process.

Figure 4 shows the variation of the parallel and perpendicular coercive force (H_c) of PVDF/Fe_3O_4 nanocomposite with the Fe_3O_4 content. However, a different variation trend of the coercive force (H_c) with the change of Fe_3O_4 content is observed. The results show that the H_c of the PVDF/Fe_3O_4 nanocomposite is mostly 80–85 Oe, and that the H_c is independent of the Fe_3O_4 content and approximately equal along the parallel and perpendicular at the same Fe_3O_4 content. When the Fe_3O_4 nanoparticles form some aggregates in the PVDF matrix, the mean interparticle distances possibly increases and the dipolar interactions decrease compared with those under the state of the uniform dispersion without aggregation, this perhaps leads to a higher anisotropy barrier and a higher H_c.[25] With the increase of Fe_3O_4 content, the mean interparticle distances further increased but may exceed the effective distance of the dipolar interactions; therefore, the anisotropy barrier and the H_c no longer increases, which results in the H_c independent of the Fe_3O_4 content. The hot-pressed processes produce the anisotropy; however, the dipolar interactions are not probably influenced due to the exceeding of the effective distance and therefore the H_c was similar along the parallel and perpendicular directions at the same Fe_3O_4 content.

Optical absorption coefficients and optical band gap analysis

The samples for UV-Vis absorption measurement are self-supporting slices. The optical absorption coefficient α is determined from the following relationship between the transmitted light I_t and the sample thickness d,[26,27]

$$I_t = I_0(1 - R)^2 \exp(-\alpha d) \quad (1)$$

where I_o and R are the incident light intensity and the reflectivity of the samples, respectively. If R is very small and can be neglected, the α can be

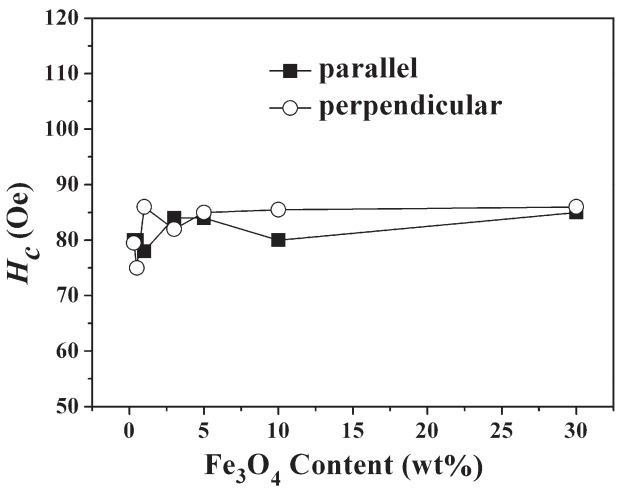

Figure 4 Variation of the parallel and perpendicular coercive force (H_c) of the PVDF/Fe_3O_4 nanocomposite slices with the Fe_3O_4 content.

obtained by the value of I_t/I_o and d. The I_t/I_o can be measured by UV-Vis spectrometer.

Figure 5 shows the variation of the α of the PVDF/Fe_3O_4 nanocomposite with photon energy at the different Fe_3O_4 content. The results show that the α augments with the increase of Fe_3O_4 content at the same photon energy, which indicates the decrease of the transparency of the nanocomposite with the increase of the Fe_3O_4 content. However, there is a bit irregularity that the α of PVDF/Fe_3O_4 nanocomposite with 1 wt % Fe_3O_4 is lower than that of nanocomposite with 0.5 wt % Fe_3O_4, and that some protuberance and big fluctuation appear in the curve of the nanocomposite with 3 wt % Fe_3O_4. These probably are related to the nonuniform dispersion of the Fe_3O_4 nanoparticles in PVDF matrices and imperfectness of the samples, resulting from the detailed preparation processes.

The theory of interband optical absorption shows that at the absorption edge the optical absorption coefficients α varies with the photon energy $h\nu$ according to the following expression,[26,27]

$$(\alpha h\nu)^n = A(h\nu - E_g) \quad (2)$$

where h is Plank constant, E_g is optical band gap, A is a constant, and n is a number that characterizes the transition process. n takes the value 2 for the direct allowed transition, 2/3 for direct forbidden, 1/2 for the indirect allowed transition, and 1/3 for the indirect forbidden. The usual method for determining the value of E_g involves plotting $(\alpha h\nu)^n$ against the photon energy $h\nu$. If the appropriate value of n has been used, the graph is a straight line, and the E_g is given by the intercept on the photon energy axis. By plotting as described in the above, the results show that 2 is an appropriate value of n for the PVDF/Fe_3O_4 nanocomposite, and thus, the $(\alpha h\nu)^2$ is plotted as a function of photon energy $h\nu$ shown in Figure 6 to obtain the optical band gap E_g. By extrapolating a linear portion of every curve in Figure 6 to $(\alpha h\nu)^2 = 0$, the direct energy gap E_g for respective PVDF/Fe_3O_4 nanocomposite with different Fe_3O_4 content can be obtained by the intercept on the photon energy axis and the results are shown in Figure 7. The error bars are brought in the processes of the extrapolating. It can be seen that the E_g only fluctuates within the range of 0.15 eV when the Fe_3O_4 content is less than 1 wt %. When the Fe_3O_4 content increases to 3 wt %, the E_g decreases by 0.75 eV compared with that of the pure PVDF. The E_g of the PVDF/Fe_3O_4 nanocomposite with higher Fe_3O_4 content can not be measured due to the opacity of the slices.

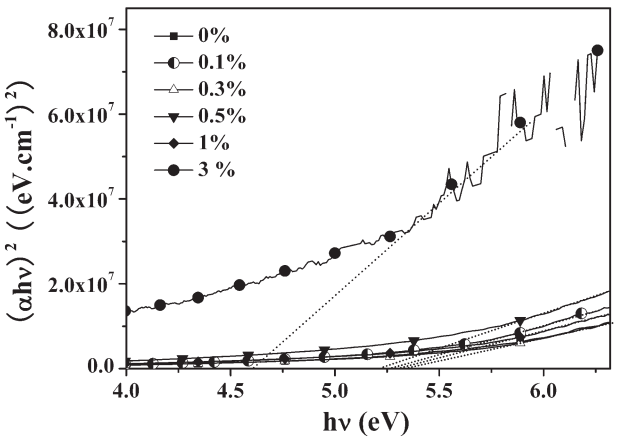

Figure 6 $(\alpha h\nu)^2$of the PVDF/Fe_3O_4 nanocomposite at various Fe_3O_4 content as a function of photon energy ($h\nu$).

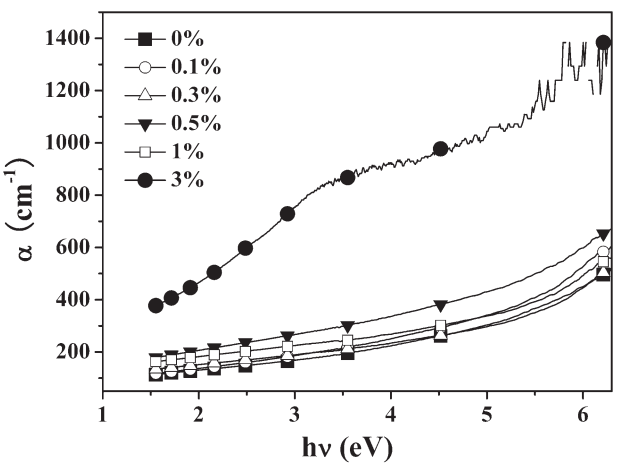

Figure 5 Optical absorption coefficients (α) of the PVDF/Fe_3O_4 nanocomposite at various Fe_3O_4 content as a function of photon energy ($h\nu$).

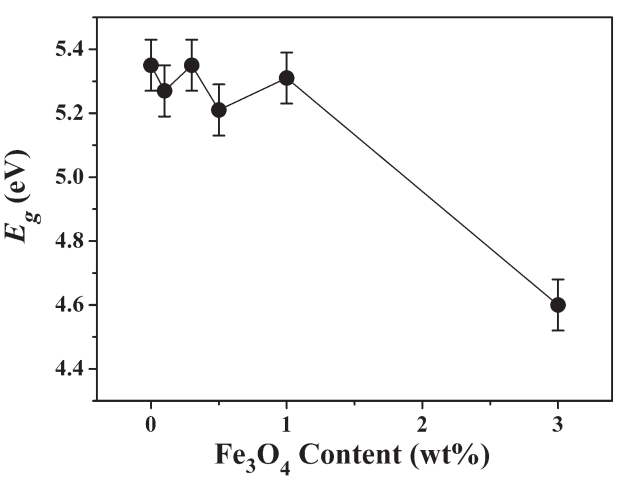

Figure 7 Optical band gap (E_g) of the PVDF/Fe_3O_4 nanocomposite as a function of the Fe_3O_4 content.

CONCLUSIONS

By a simple coprecipitation method, PVDF/Fe_3O_4 magnetic nanocomposite was prepared with the aid of the sonication. The Fe_3O_4 nanoparticles formed some 50 nm–5 μm conglomerates in the PVDF matrices, and the sizes of these conglomerates increased with the increase of Fe_3O_4 content. The Fe_3O_4 nanoparticles retained their phase structure in the nanocomposite but decreased the crystallinity of the PVDF. The saturation magnetization (M_s) and remnant magnetization (M_r) of the PVDF/Fe_3O_4 nanocomposite showed an increasing trend with the increase of Fe_3O_4 content, but the values along the parallel direction were higher than that of the perpendicular at the same Fe_3O_4 content. The coercive force (H_c) was independent of the Fe_3O_4 content and approximately equal along the parallel and perpendicular direction. The optical band gap (E_g) of the PVDF/Fe_3O_4 nanocomposite was influenced by the Fe_3O_4 content and decreased by 0.75 eV compared with that of pure PVDF when the Fe_3O_4 content was 3 wt %. Further investigation on the nature and mechanism of the magnetic and optical properties is ongoing and to be reported in the following articles.

The authors are very grateful to Professor Zhengjun Zhang and Professor Zhengcao Li for their help and discussion, Professor Yunhan Ling, Professor Ming Li, and Professor Cewen Nan for their help in preparation processes.

References

1. Wei, S. S.; Zhu, Y. F.; Zhang, Y. J.; Xu, R. React Funct Polym 2006, 66, 1272.
2. Qiu, G. H.; Wang, Q.; Nie, M. J Appl Polym Sci 2006, 102, 2107.
3. Deng, Y. H.; Yang, W. L.; Wang, C. C.; Fu, S. K. Adv Mater 2003, 15, 1729.
4. Ding, X. B.; Sun, Z. H.; Wan, G. X.; Jiang, Y. Y. React Funct Polym 1998, 38, 11.
5. Gomz-Lopera, S. A.; Plaza, R. C.; Delgad, A. V. J Colloid Interface Sci 2001, 240, 40.
6. Okubo, M.; Minam, H.; Komura, T. J Appl Polym Sci 2003, 88, 428.
7. Lindla, B.; Boldt, M. Adv Mater 2002, 14, 1656.
8. Xulu, P. M.; Fillipcsei, G.; Zrinyi, M. Macromolecules 2000, 33, 1716.
9. Matsuno, R.; Yamamoto, K.; Otsuka, H.; Takahara, A. Macromolecules 2004, 37, 2203.
10. Chen, A. H.; Wang, H. Q.; Zhao, B.; Li, X. Y. Synth Met 2003, 139, 411.
11. Chen, A.; Wang, H.; Zhao, B.; Wang, J.; Li, X. Acta Mater Compos Sin 2004, 21, 157.
12. Qiu, G. H.; Wang, Q.; Wang, C.; Lau, W.; Guo, Y. L. Ultrason Sonochem 2007, 14, 55.
13. Kaise, A. B.; Subramaniam, C. K.; Gilberd, P. W.; Wessling, B. Synth Met 1995, 69, 197.
14. Lee, D. K.; Kang, Y. S.; Lee, C. S.; Stroeve, P. J Phys Chem B 2002, 106, 7267.
15. Chen, C. X.; Qian, S. M.; Gong, F. F.; Wang, Z. H.; Jiang, J. S.; Yang, X. L. Chin J Mater Res 2000, 14, 334.
16. Ennas, G.; Musinu, A.; Piccaluga, G.; Zedda, D.; Gatteschi, D.; Sangregorio, C.; Stanger, J. L.; Concas, G.; Spano, G. Chem Mater 1998, 10, 495.
17. Ma, H.; Jen, A. K.; Dalton, L. R. Adv Mater 2002, 14, 1339.
18. Asano, T.; Kubo, T.; Nishikitani, Y. J Photochem Photobio A: Chem 2004, 164, 111.
19. Anandan, S.; Pitchumani, S.; Muthuraaman, B.; Maruthamuthu, P. Sol Energy Mater Sol Cells 2006, 90, 1715.
20. Dillon, D. R.; Tenneti, K. K.; Li, C. Y.; Ko, F. K.; Sics, I.; Hsiao, B. S. Polymer 2006, 47, 1678.
21. Moussaif, N.; Groeninckx, G. Polymer 2003, 44, 7899.
22. JCPPS Power Diffraction File International Center for Diffraction Data, Fe_3O_4, Newtown Square, PA 1980.
23. Zhou, J.; Ma, M.; Zhang, Y.; Gu, N. J. Nat Sci Ed (Southeast Univ) 2005, 35, 615.
24. Dormann, J-L.; Fiorani, D.; Tronc, E. Adv Chem Phys 1997, 98, 283.
25. Baker, C.; Ismat Shah, S.; Hasanain, S. K. J Magn Magn Mater 2004, 280, 412.
26. Toyoda, T.; Nakanishi, H.; Endo, S.; Irie, T. J Phys D: Appl Phys 1985, 18, 747.
27. Toyoda, T.; Maruyama, S.; Nakanishi, H.; Endo, S.; Irie, T. J Phys D: Appl Phys 1986, 19, 909.